DVCS inner calorimeter prototype calibration

I. Bedlinskiy[1], V. Kubarovsky[2]
S. Kuleshov[1], O. Pogorelko[1]

[1]ITEP, Moscow
[2]RPI

November 17, 2004

Abstract

The lead-tungsten electromagnetic calorimeter has been tested in the Hall B electron beam. The prototype has been built with 100 tappered crystals. Each crystal has dimensions of 13.3x13.3 mm(front face), 16x16 mm(rear face) and 160 mm length. Three different methods were used for the calorimter calibration: laser light, quasi-elastic electron scattering off carbon nuclei, and $\pi^0 \to \gamma\gamma$ decay. It was shown that calibration procedure based on the π^0-mass constrain in the decay $\pi^0 \to \gamma\gamma$ is very promising.

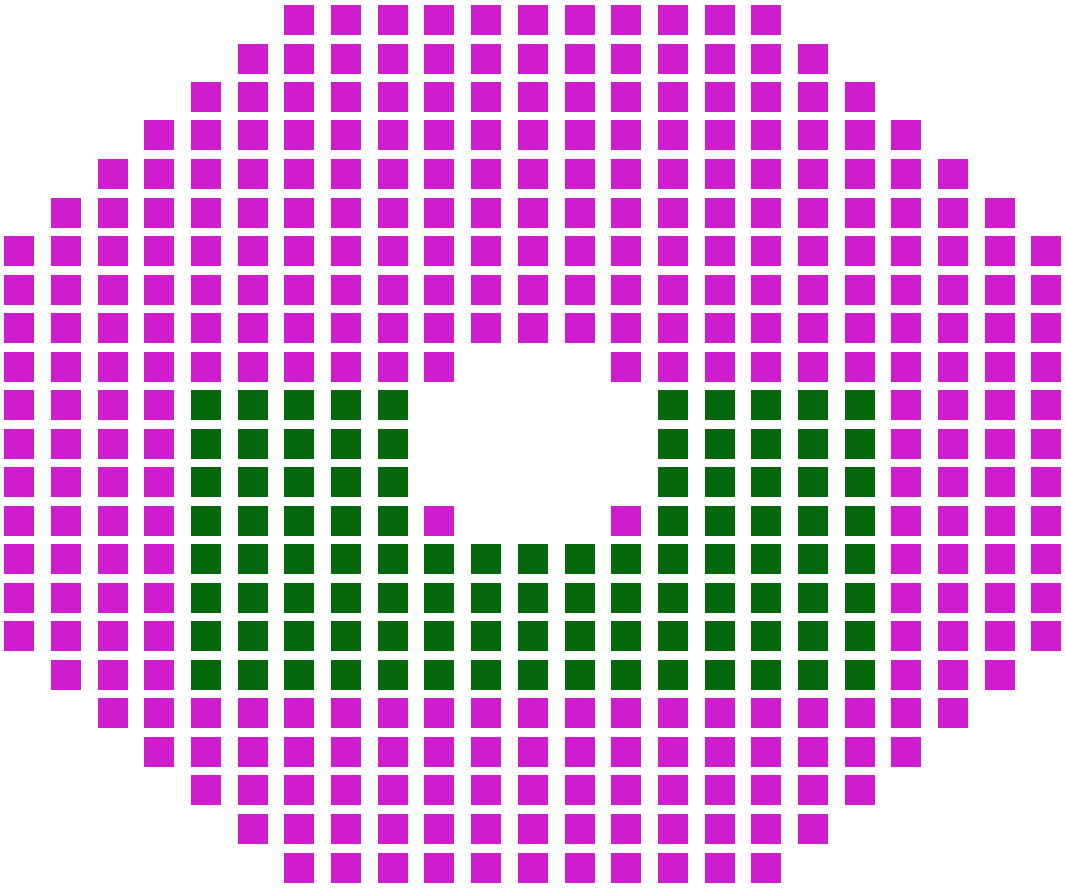

Figure 1: DVCS Inner Calorimeter. Crystals used in the prototype are represented by green color

1. Introduction

The prototype includes 100 tapered lead-tungsten crystals with dimensions of 13.3x13.3 mm^2 (front face), 16x16 mm^2 (rear face), 160 mm (length) and readout system - Hamamatsu avalanche photodiodes (5x5 mm^2 window) and 100 low noise amplifiers (Fig.1, dark green). The final version of the Inner Calorimter(IC) will consists of 424 crystals[1]. The electron beam of the Hall B with energy 5.0 GeV was used for the test. Electrons interacted with carbon target C^{12}(2.7 mm length) located at the distance of 60 cm from the front face of the calorimeter. In this data analysis only IC trigger events were used[2].

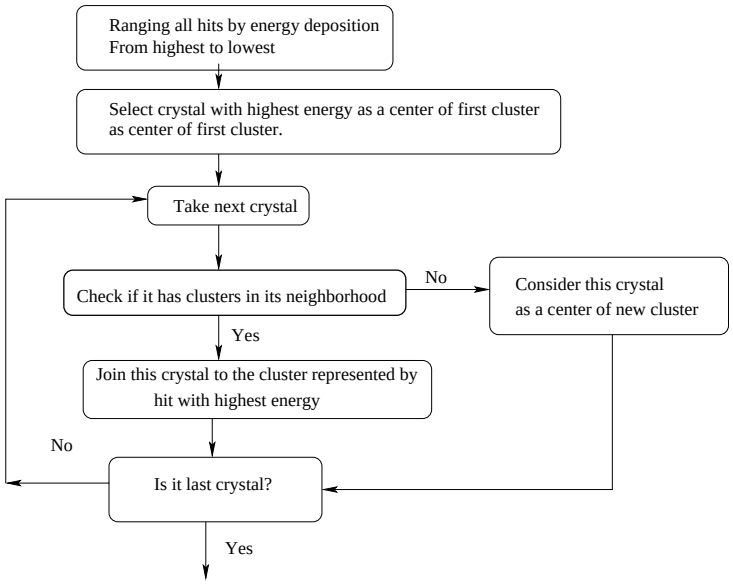

Figure 2: Algorithm of the cluster reconstruction.

2. Clusters reconstruction

Cluster reconstruction algorithm is shown on Fig. 2 Hit is the energy deposition in a single crystal with the amplitude more than threshold (5 MeV). Cluster is an event with number of hits ≥ 1, and one or more hits must have amplitude more than threshold (60 MeV).

To reconstruct clusters the following procedure was used:

- Sorting all hits by energy deposition from highest to lowest.
- Selection of the crystal with the highest energy deposition and declaration it to be a center of the first cluster.
- Forming cluster
  - Checking the second hit location as a neighbor (eight crystals) relative to the first hit.
  - If the next hit has no neighbors it is a center of the next cluster.

The example of the reconstructed clusters is shown in Appendix 1.

X and Y position of the cluster center are determined via logarithmic weighting of clusters:

$$x = \frac{\sum x_i W_i}{\sum W_i}, \qquad (1)$$

where x_i and W_i are the position and the logarithmic weight of the crystal i. The fraction of the cluster energy contained in the crystal was calculated with the formula[3]:

$$W_i = W_0 + log(\frac{E_i}{\sum E_j}), \qquad (2)$$

where $W_0 (W_0 = 3.1)$ was selected with GEANT optimization. It controls the smallest fraction energy in a crystal, that can contribute to the position measurement.

The described procedure has some disadvantages:

- No corrections for the boundary effects of the calorimeter.
- No corrections for bad channels in the calorimeter.
- The the reconstruction and resolution of close and overlapping clusters was not optimized.
- No corrections for energy losses in gaps between crystals.

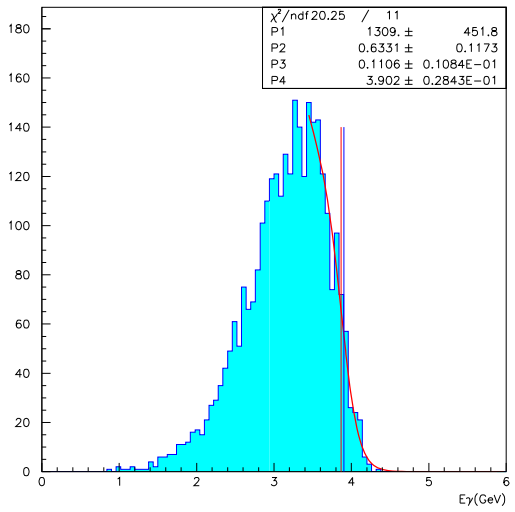

Figure 3: Energy deposition for the central hit of the cluster.

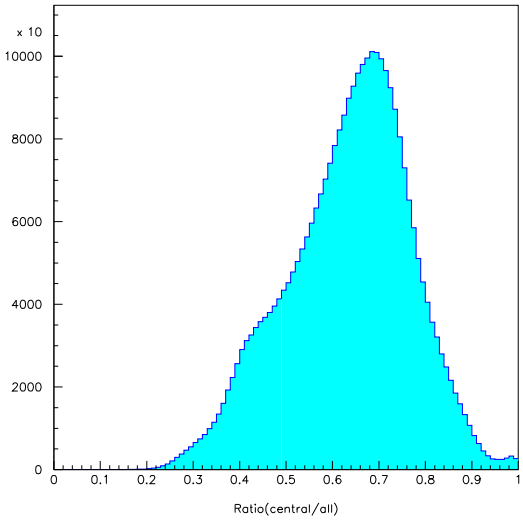

Figure 4: Ratio of energy deposition in central hit to the full cluster energy

3. Quasi free electron scattering calibration

The preliminary channel calibrations with laser monitoring system were provided [2]. The simplest way to calibrate the calorimeter is using exclusive process of quasi-free electron scattering off single nucleon of a target. From a basic kinematic calculations it is known that electron scattered at some angle via quasi free mechanism always has higher energy than similar electron from any non-elastic reaction. The energy distribution of the central crystal of the cluster is shown on Fig. 3. The right edge of the energy distribution corresponds to quasi-elastic electron scattering. Right edges of the energy distribution of all operating crystals were fitted by special function . The following procedure was used to select quasi free electron scattering:

1. Selection of events with single high energy cluster in the calorimeter.
2. Selection of clusters with 4 hits or more.
3. Selection of the central hits for each cluster for calibration of crystals.

The highest energy deposition in the hit corresponds to the scenario when particle hits crystal in the center, and the ratio of energy deposition in single crystal to the energy deposition in entire crystal is 0.7(Fig 4). Later GSIM simulation was made for eleastic electron scattering on hydrogen target with C^{12} target geometry. The average energy deposition in each crystal was obtained.

The energy of electron scattered off nucleon at given angle is:

$$\mathrm{E}=\frac{E_0}{1+\frac{2E_0}{m}*sin^2(\theta/2)}, \qquad (3)$$

where E - is the energy of scattered electron, E_0 - is the energy of the initial electron, θ- is the angle of the scattered electron.

For the selected events the energy distribution in the single crystal (only after laser calibration) is shown on Fig. 3. This distributions were fitted by the function:

$$f(x)=\frac{P1*e^{-P2*x}}{1+e^{\frac{x-P4}{P3}}}, \qquad (4)$$

where P1, P2, P3, P4 - parameters of the fit

Parameter P4 of the fit corresponds to the vertical line on this distribution. This method is not completely correct for data of the DVCS IC prototype test, because the target used during this run was C^{12} and scattering off nucleons involved in Fermi motion. For DVCS run with H^2 target this method will work better.

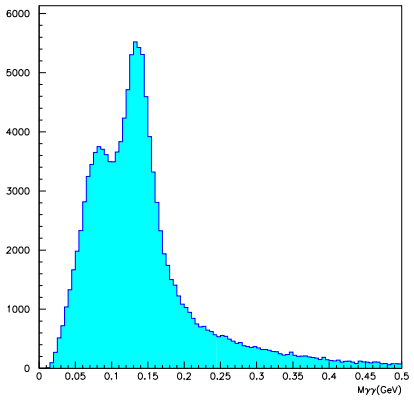

Figure 5: $M_{\gamma\gamma}$ invariant mass after first 2 cuts.

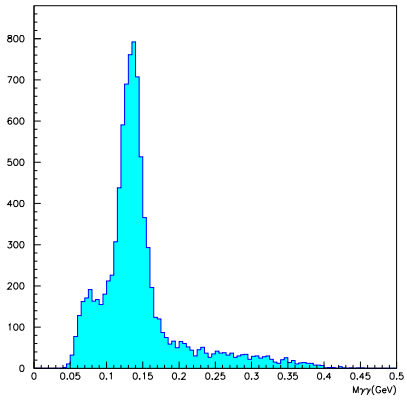

Figure 6: $M_{\gamma\gamma}$ invariant mass after all cuts.

4. π^0 Clusters calibration

The $\pi^0 \rightarrow \gamma\gamma$ decay was used for the energy calibration of the electromagnetic calorimeter. Both γ-s hit the inner calorimeter. Also it was assumed that π^0 decay vertex is located in the center of the solid target. Conditions for cuts are described below. First two cuts were always used, the other three cuts were used as additional strong cuts.

1. Only events with two and only two clusters in the calorimeter were selected.
2. Both clusters are "good". The requirements for "good" clusters are listed below:
   - The energy deposition in the center crystal has to be $E_{crystal} > 100MeV$.
   - Central crystal is not located on the edge of the calorimeter (this requirement does not allow to use π^0 for border crystals). Not operating channels create "holes" and disturb the calibration.
   - The ratio of energy deposition in the central crystal to the total energy of the cluster has to be: $R = \frac{E_{centralcrystal}}{E_{total}} > 0.4$
3. At least one cluster has energy $E > 1.5$ GeV.
4. Total energy of every cluster must be $E_{total} > 0.6$ GeV
5. Total energy of two clusters is within a range 2.1 GeV$> E_{\gamma\gamma} > 3.0$ GeV

On Fig. 5, 6 the invariant mass spectra $M_{\gamma\gamma}$ with cuts 1 and 2 and cuts 1-5 are shown. $\pi 0$ peak is clearly seen in both distributions. With additional cuts 1-5 distribution gets cleaner (Fig. 6). 2D plots E_γ, distance between clusters, $E_{\gamma\gamma}$ vs $M_{\gamma\gamma}$ are presented on Figs. 7, 8, 9 respectively.

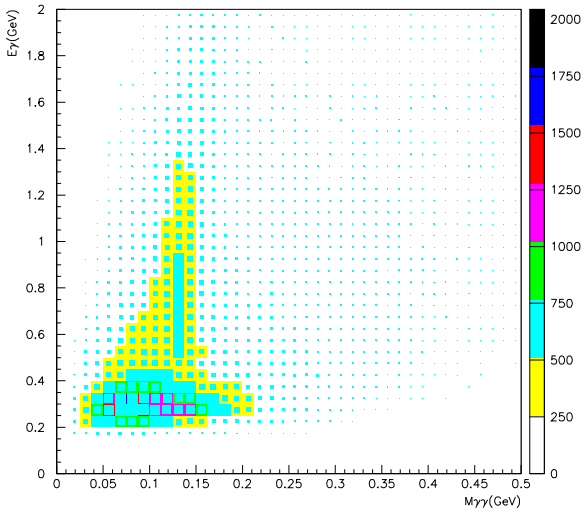

Figure 7: Dependence of the cluster energy E_γ (lower energy from two clusters) vs $M_{\gamma\gamma}$

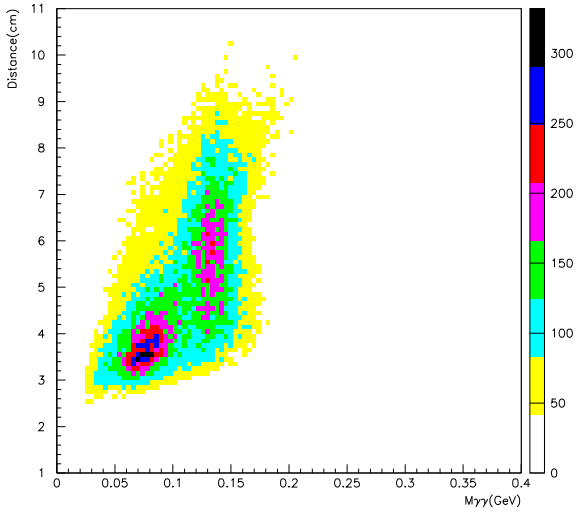

Figure 8: Distance between two clusters vs $M_{\gamma\gamma}$, cuts 1,2 applied.

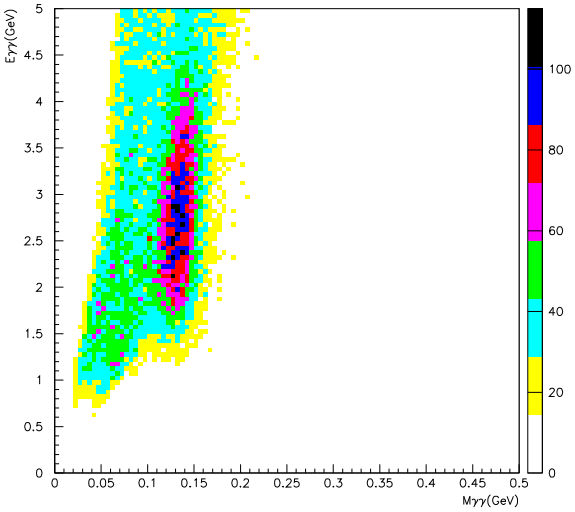

Figure 9: $E_{\gamma\gamma}$ vs $M_{\gamma\gamma}$, cuts 1-2 applied.

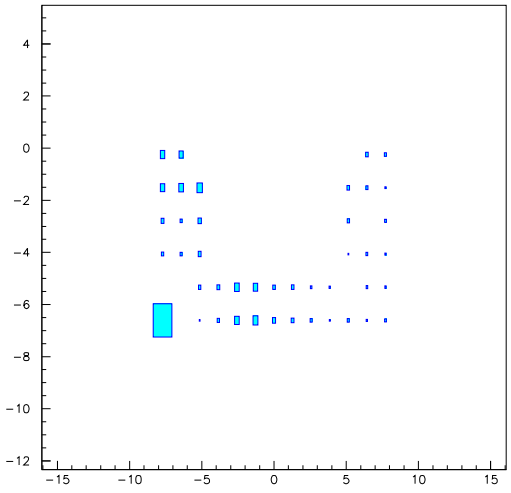

Figure 10: Calorimeter occupancy with fixed cluster center.

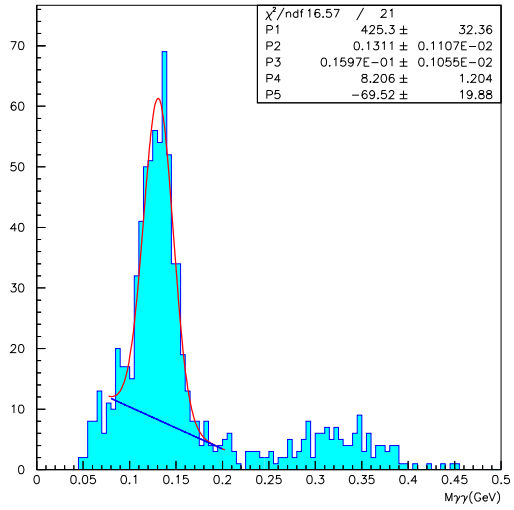

Figure 11: $M_{\gamma\gamma}$ with fixed cluster center.

5. Calibration of crystals

Boundary crystals can not be calibrated as well as problematic crystals within the calorimeter. Only crystals that contain centers of clusters could be calibrated. To calibrate the crystal all pairs of clusters were selected where the center of one cluster is located in this crystal. Plot of cluster centers of all pairs , when one of clusters centers is fixed and second is free is shown on Fig. 10. Holes on the occupancy plot due to not operating channels can also be seen. The example of the $M_{\gamma\gamma}$ distribution is shown on Fig. 11

The position of this peak is determined by the equation

$$M^2_{\gamma\gamma} = 2E_1E_2\sin^2\alpha, \qquad (5)$$

where E1, E2- energies of 1st and 2nd clusters respectively.

This peak position can be used for adjustments of calibration constants, initially obtained from laser calibration and/or right edge calibration. The iteration method was used for calibration. Constant correction coefficient was calculated at each iteration step using formula:

$$C(i) = \frac{1.5M_{\pi^0}}{M_{peak(i)}} - 0.5, \qquad (6)$$

where C(i)- is correction coefficient, $M_{peak(i)}$- is mass peak position.

One peak was used to correct one constant at every iteration. Coefficient 1.5 means that energy deposition in central crystal is about 0.7 of total cluster energy.

The calibration constants are shown on Fig. 12. The systematic shift of constants can be attributed to ratio of the energy deposition in the central channel to the deposition in the entire cluster in the right edge calibration and to the systematic error to the angle between clusters introduced by cluster reconstruction in the case of π^0 calibration. The reconstructed invariant mass $M_{\gamma\gamma}$ for each crystal are shown on Fig. 13

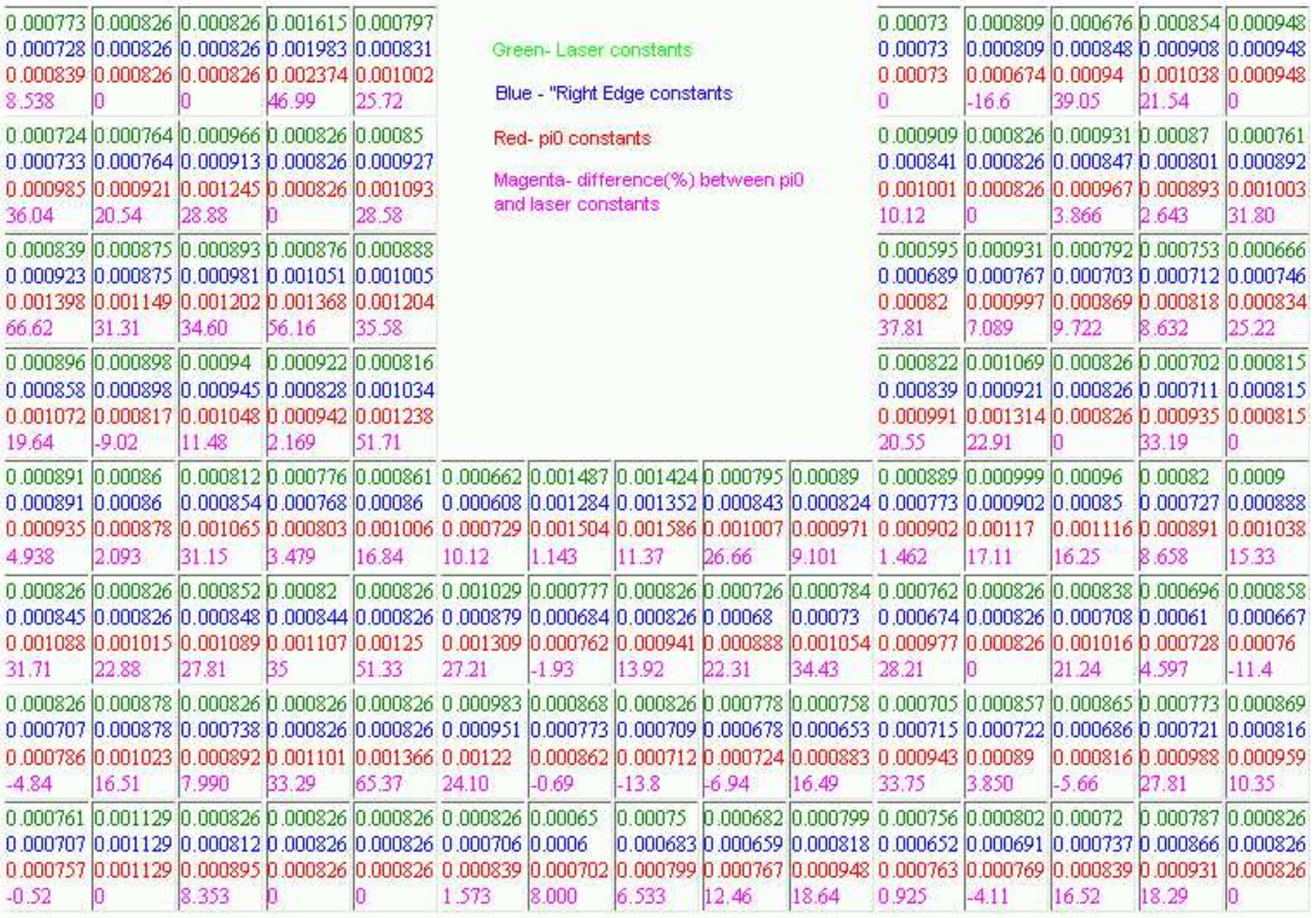

Figure 12: Calibration constants.

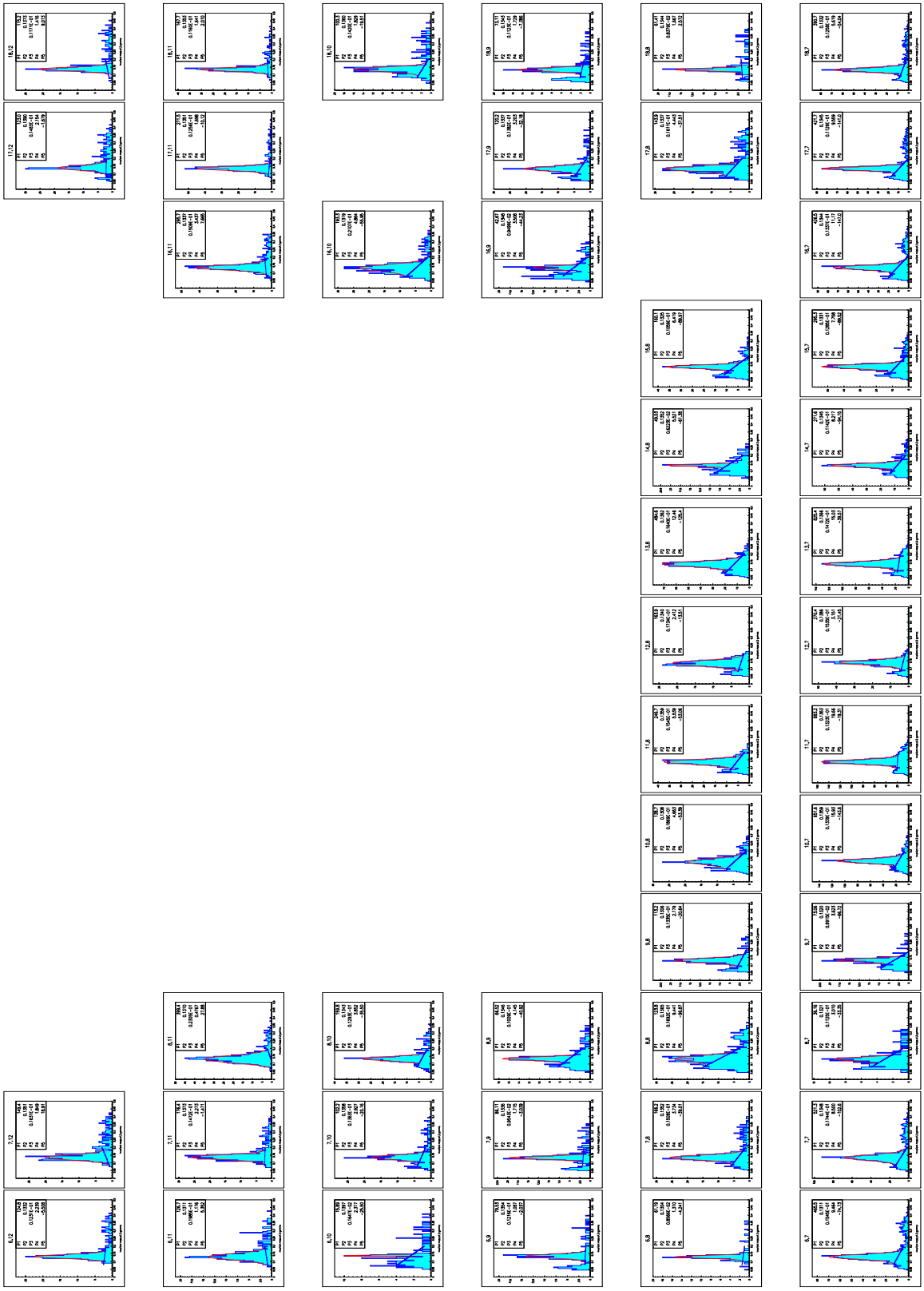

Figure 13: Reconstructed $M_{\gamma\gamma}$.

Conclusions

1. Laser calibration and right edge of quasi-elastic peak calibration of the channels allow pick out photons from π^0 decays.

2. $\gamma's$ from π^0 decays allow to provide absolute energy calibration of the calorimeter during long time runs alter irradiation degradation of the light output of lead-tungsten crystals and laser monitoring system.

3. More studies of localization of the electromagnetic showers must be provided.

References

1. CLAS Proposal E-01-113 for DVCS calorimeter.

2. CLAS NOTE 2004 DVCS electromagnetic calorimeter prototype test results, not published.

3. CMS Note 2001 "Electron Reconstruction in the CMS Electromagnetic calorimeter", E. Meishi, T. Monteiro, C. Seez and P. Vikas

Appendix 1